*Journal of Nepal Geological Society, 2023, Vol. 65 (Sp. Issue), pp. 71–88*
https://doi.org/10.3126/jngs.v65i01.57753

# Strength and durability status of the Fagfog Quarzite from the Lower Nawakot Group, central Nepal Lesser Himalaya

**Dinesh Raj Sharma and Naresh Kazi Tamrakar***

*Central Department of Geology, Tribhuvan University, Kirtipur, Kathmandu, Nepal*
**Corresponding author's email: nktam555@gmail.com*

## ABSTRACT

Railways have played vital role in the development of many countries worldwide. Government of Nepal has already planned to establish various national and international railway networks within the nation. A substantial quantity of durable rock ballasts is required for building a sustainable railway network. Quartzites from central Nepal Lesser Himalaya can be a promising source to fulfill this requirement. Therefore, the quartzites from the stratigraphic unit Fagfog Quartzites of the Lower Nawakot Group located in Dhading District along the Kalu Pandey Highway have been assessed to determine physical, strength and durability characteristics of the ballasts. All quartzite ballasts obtained from the bedrocks were of Precambrian, medium-grained, bladed to prolate shaped, white to brownish white, crushed quartzites. Dry density and water absorption were respectively 2336-2641 kg/m$^3$ and 0-2.5%. The bulk density varies from 1204 and 1387 kg/m$^3$. Point load strength index varies from 2.04 to 11.55 MPa (medium strong to extremely strong). Aggregate impact value (AIV) and aggregate crushing value (ACV) ranges from 14.85 to 22.77% and 15.51 to 22.17% respectively. Some 7% results of AIV and 20% of ACV results exceeded the established limiting value of 22%. The slake durability index ($I_{d5}$) ranges from 95.19 and 99.11%, whereas $I_{d_2}$ ranged between 96.94 and 100%, which shows that 80% of the samples have very high slake durability whereas remaining 20% exhibit high slake durability. There was no significant change in slake durability index from the second to the fifth cycles. Los Angeles Abrasion Value (LAAV) varies from 12.07 to 31.34% and sulphate soundness value (SSV) varies within a limited range of 0.20 and 4.59%. Conclusively, the comprehensive evaluation suggests that the quartzite ballast from the Fagfog Quartzite source display favourable qualities in terms of point load, crushing and impact strengths and durable against abrasion, slaking and frosting. Thus, the quartzites from Fagfog Quartzite hold significant potential as a suitable rock type for railway track ballasts.

**Keywords:** Railway track ballast, quartzite, strength of ballasts, slake durability index, Los Angeles abrasion

**Received:** 24 January 2023 **Accepted:** 05 June 2023

## INTRODUCTION

The most crucial and significant characteristics of rock are strength and durability. Strength and its associated measures are point-load strength index (PLSI), aggregate crushing value (ACV) and aggregate impact value (AIV) that respectively measure strength, resistance to crushing and resistance to impact. Durability, meaning weathering in number of cycles (temporal weathering) and abrasion and impact of individual rock types give indication of long-term durability of rocks, and it may differ due to variation in rock types and fabric. Slake durability index (SDI), Sulphate Soundness value (SSV), and Los Angeles abrasion value (LAAV) are widely used durability measures to characterize durability against slaking, freeze and thawing, and abrasion (Gökçeoğlu et al., 2000; Erguler and Ulusay, 2009; Gautam and Shakoor, 2013). Strength and durability tests are made to distinguish clearly between the superior and inferior quality of construction materials. Both strength and durability are the determining factors when assessing rock for various applications (Ahmada et al., 2017).

Several researchers examined the physical and mechanical characteristics of the rocks from the Lesser Himalaya and the Sub-Himalaya to show how they may be used as aggregates (Tamrakar et al., 2002; Maharjan and Tamrakar, 2003; Dhakal et al., 2006; Khanal and Tamrakar, 2009). Gupta and Sharma (2012) investigated quartzites from the northwest Himalayas and came to the conclusion that texture and rock strength were closely correlated. Quartzites are one of the most strong and durable rock types (Maharjan and Tamrakar, 2007; Bista and Tamrakar, 2015). They are therefore suitable rock types for construction aggregates and stones because they perform well under severe weathering environment and heavy load. Therefore, present study primarily aims to investigate strength and durability characteristics of some of the quartzites from the Fagfog Quartzite of the Lower Nawakot Group (Stöcklin, 1980) from Dhading District of central Nepal, mainly for railway track ballast.

## GEOLOGICAL SETTING

The Lesser Himalaya of central Nepal is bounded by the Main Central Thrust in the north and the Main Boundary Thrust in the South. It comprises mainly of sedimentary to metasedimentary rocks like slate, phyllite, quartzite, limestone, dolomite, sandstone, etc. (Stöcklin and Bhattarai, 1977). The Lesser Himalayan stratigraphic units are distinguished into the autochthonous Nawakot Complex and the allochthonous Kathmandu Complex. The Nawakot Complex is divided into the Lower Nawakot Group and the Upper Nawakot Group

(Stöcklin and Bhattarai, 1977; Stöcklin, 1980). The current field study is located in the Bangchung-Kalidaha along the road section from Dhading to Malekhu (Fig. 1). The Kuncha Formation, Fagfog Quartzite, Dandagaon Phyllite, Nourpul Formation, and Dhading Dolomite from the oldest to the youngest units of the Lower Nawakot Group are well exposed along this road section. Strata strike NW-SE and are overturned dipping towards the north.

## METHODOLOGY

Stratified selective samples of quartzites were taken as grab samples from the Fagfog Quartzite exposed at the portion of the Kalu Pandey Highway between Kalidaha and Bungchung (Fig. 2). Sampling horizons are indicated in Figure 3. Information on sampling location, and rock texture and structure was recorded during sampling.

The required amount of samples was brought to the material testing laboratory for further tests. Thin slices of quartzite were prepared to study under the polarizing microscope. Test samples from the individual samples were prepared for desirable tests; physical properties, strength and durability.

### Test for physical properties

#### *Shape Indices*

Shape indices are attributed by flakiness index (FI) and elongation index (EI). Both FI and EI were determined following BS 812 105.1 (1989) and BS 812 105.2 (1990). FI was determined for 50 mm down to 37.5 mm and 37.5 mm down to 25 mm aggregates using a thickness gauge in which aperture size is 0.6 times the average of passing and retained sizes of aggregate to be tested. The Equation 1 was used to compute FI.

$$Flakiness\,Index = \frac{X_1 + X_2 + X_3 ..... X_n}{W_1 + W_2 + W_3 ..... W_n}.100 \qquad (1)$$

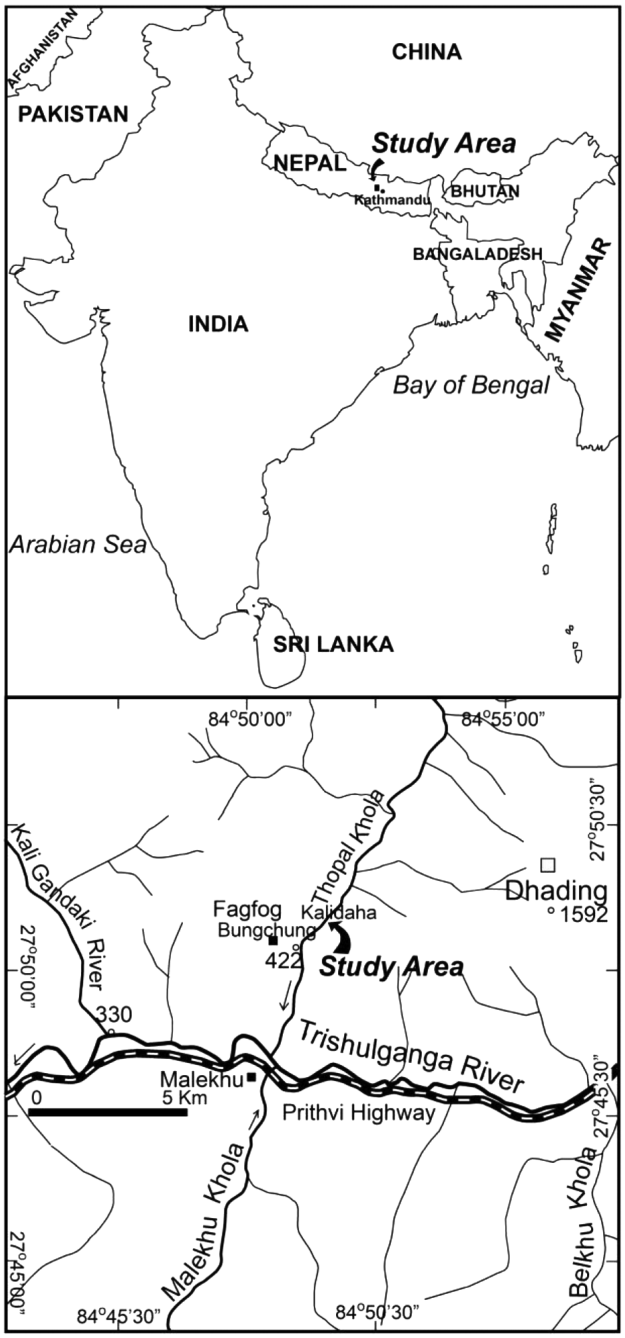


**Fig. 1: Location of study site, east of Fagfog and near the Thopal Khola.**

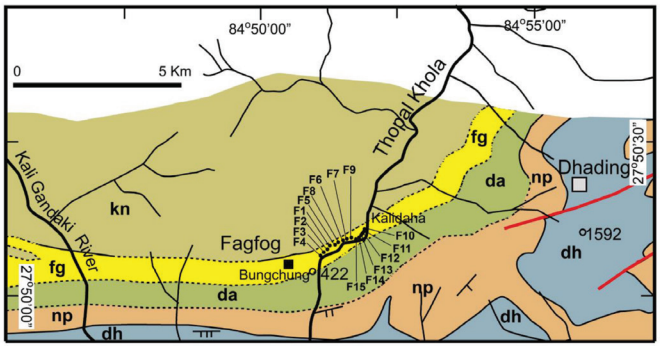


**Fig. 2: Regional geological map of the study area. kn=Kuncha Formation, fg=Fagfog Quartzite, da=Dandagaon Phyllite, np=Nourpur Formation, dh=Dhading Dolomite (after Stöcklin and Bhattarai 1977), F1 to F15 are sampling sites.**

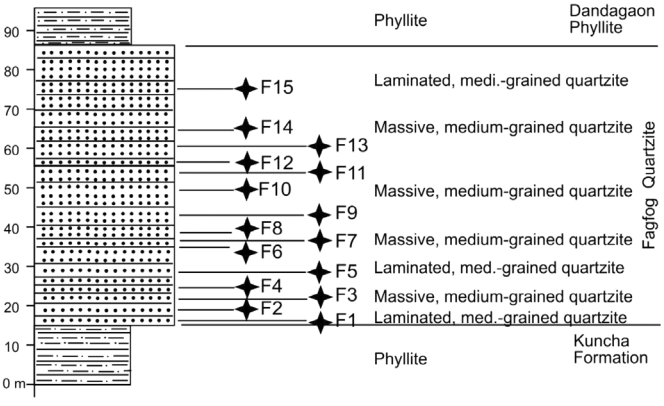


**Fig. 3: A columnar section of Fagfog Quartzite at the Kalu Pandey Highway between Kalidaha and Bungchung in the Thopal Khola area (See Fig. 2 for location).**

where, X denotes weight of the fraction passing through the thickness gauge and W denotes the weight of the original sample on the corresponding sieve size.

*Elongation index*: Aggregate particles are classified as elongate when they have a length (greatest dimension) of more than 1.8 of their mean sieve size. The elongation index was determined by separating aggregates which fail to pass through an elongation gauge. EI was calculated using the Equation 2.

$$Elongation\,Index = \frac{Y_1 + Y_2 + Y_3 ..... Y_n}{W_1 + W_2 + W_3 ..... W_n} .100 \quad (2)$$

Where, Y denotes the weight of the fractions retained on the length gauge and W denotes the weight of the original sample retained as the corresponding sieve.

***Specific gravity, density and water absorption***

The laboratory procedures for specific gravity and water absorption were followed according to ASTM C127 (2011). The test sample was oven dried at constant mass at a temperature of 110±5°C. The oven dry (OD) mass of sample was recorded. Subsequently, the sample was immersed in water at room temperature for 24 hr. Then it was removed and was soaked by moist cloth until all visible films of water were removed. At this stage the saturated surface dry (SSD) mass of the sample was recorded. The SSD sample was then immersed in water removing all entrapped air by shaking the container when immersed. The apparent mass of the sample was measured in water. The following equations (3–5) were used to compute, specific gravity of oven dried sample ($G_{OD}$), Density of oven dried sample ($D_{OD}$) and water absorption (WA).

$$G_{OD} = \frac{A}{(B - C)} \quad (3)$$

$$D_{OD} = 997.5 \frac{A}{(B - C)} \quad (4)$$

$$WA = \frac{(B - A)}{(A)} .100 \quad (5)$$

where, A is the mass of oven-dried test sample in air (in kg), B is the mass of saturated- surface-dry test sample in air (kg), and C is the apparent mass of saturated test sample in water (kg).

***Bulk density***

When aggregates are packed in a given volume of space, the volume of space not only contains aggregates but also void spaces among particles. Therefore, bulk density takes into account of both aggregates and void spaces in a given volume. It is also a measure of how well packed the aggregates are in the given space. Bulk density of ballasts was determined following ASTM C 29/C 29M – 07 (2007) by rodding the ballast in a measure. The dry bulk density for rodding was calculated using the following relation (Eq. 6):

$$Bulk\ density = \frac{(G - T)}{(V)} \quad (6)$$

where, G is the oven dry mass of sample plus the measure (kg), T is mass of the measure (kg), and V is the volume of the measure ($m^3$).

**Strength test**

***Point load strength index test***

Point load strength index (PLSI) test is intended as an index test for the strength classification of rock material (Broch and Franklin, 1972). Irregular lumps with its width and thickness measured and tabulated, were used in this test following the procedure of ASTM D5731–02 (2003). Irregular lumps were loaded normal to the stratification, and the breakage load was recorded in KN. The PLSI that is denoted by symbol $I_s$ was calculated using the Equation 7.

$$I_s = \frac{P}{(De^2)} \quad (7)$$

where, P is a failure load (KN), and De is equivalent core diameter (m).

The equivalent core diameter is found out using the following expression (Eq. 8).

$$De^2 = \frac{4A}{\pi} \quad (8)$$

where, A is a minimum cross-sectional area of plane through the platen contacts points. The A was obtained from the products of average width and average thickness of the lump measured at least at two lines. The standard point load strength index, $I_{s(50)}$ was obtained by the product of size correction factor and point load strength index, $I_s$, using the following expression (Eq. 9).

$$I_{s(50)} = \left(\frac{D_e}{50}\right)^{0.45} I_s \quad (9)$$

For the purpose of classification of strength of intact rocks, uniaxial compressive strength (UCS) was calculated applying the following relation (Eq. 10).

$$UCS = 24\ I_{s(50)} \quad (10)$$

***Aggregate impact test***

The aggregate test sample of size between 12.5 mm and 9.5 mm and weight of about 500 g was prepared according to BS 812-112 (1990), and was filled in a cylindrical holder, one-third at a time and tamped 25 times with a tamping rod. The test sample was then fixed in position at the base of the impact machine. The test-sample was subjected to a total of 15 blows by the 14 Kg weight of hammer, each being delivered at an interval of not less than one second. The crushed aggregate was then removed and sieved on the 2.36 mm sieve. AIV was then calculated using the following expression (BS 812-112, 1990) (Eq. 11).

$$AIV = \frac{M_1 - M_2}{M_1} .100 \quad (11)$$

where, $M_1$ is the initial weight of aggregate sample, and $M_2$ is the weight of aggregate retained on 2.36-mm sieve.

***Aggregate crushing test***

The aggregate crushing value (ACV) provides a relative measure of resistance to crushing under gradually applied compressive load. It was determined after BS 812-110 (1990). About 3 kg of sample of aggregate between 12.5 mm and 9.5 mm were put in cylindrical holder at three stages slightly tamping 25 times at each stage. A plunger was inserted on to the holder in leveled position. The cylinderwith the test sample and plunger in position was placed on a compression testing machine. The load was applied in such a way to achieve 400 kN load at 15 minutes. As soon as the load was achieved, the crushed aggregate including the crushed portion were removed from the cylinder and was sieved on a 2.36-mm sieve. The ACV was calculated by using the following formula (Eq. 12).

$$ACV = \frac{W_1 - W_2}{W_1}.100 \quad (12)$$

where, $W_1$ = 3 kg is the initial weight of the dry sample, $W_2$ is the weight of the aggregate retained on 2.36 mm sieve.

**Durability test**

***Slake durability test***

Durability of rocks against cyclic wetting in water and drying is measured by the slake durability index (SDI). The SDI test is often carried as an index test for two cycles of wetting and drying and the standard value is reported. ASTM D4644-87 (1992) was followed to carry out SDI test to report standard SDI at second cycles, $I_{d2}$. Furthermore, three more cycles were added to see deterioration behavior of samples. Therefore, in total of five cycle-test was adopted. The test sample for each of the sample was of 10 pieces of lumps weighing between 40 and 60 g of each piece, and 450 and 550 g of each test sample. All the corners of the lump were smoothened and dust particles were brushed out before testing. Initially, the sample fragments were weighed and dried in the oven for 16 hours and allowed to cool at room temperature for 20 minutes, and weighed again. Thus the natural water content was calculated using the following expression (Eq. 13).

$$W = \frac{A - B}{B}.100 \quad (13)$$

where, W is the percentage of water content, A is the mass of sample at natural moisture content (g), and B is the mass of oven-dried sample before the first cycle (g).

The lump test sample was inserted in a drum and the drum with the test sample too was mounted in the trough filled with distilled water at room temperature to the level of 20 mm below the drum axis. The drum was rotated at 20 rpm for a period of 10 minutes. Afterwards, the test samples was removed from the drum to dry in the oven for 16 hours at 105° C. After cooling, the sample was weighed to obtain the oven-dried mass for the second cycle. Again the cycle was repeated to measure the weight of the sample to obtain a final mass. The tested samples were retained to evaluate disintegration. The $I_{s2}$ was computed as follows.

$$I_{d2} = \frac{W_2}{B}.100 \quad (14)$$

where, $I_{d2}$ = slake durability index (second cycle), B= mass of oven-dried sample before the first cycle in gram, and $W_2$= mass of oven-dried sample retained after the second cycle, in gram.

For assessing disintegration behaviour, samples at the end of the second cycle were tallied with Type 1, Type 2 and Type 3 patterns (ASTM D4644-87, 1992), and tabular data and graphical plots of 5-cycles were analysed.

***Sulphate soundness test***

The sulphate soundness test was carried out on the aggregate samples to determine the durability of aggregate against physical weathering. The test was done as per the standard procedure of determining the sulphate soundness of aggregates as ASTM C88–05 (ASTM International, 2005). The test sample of two kg of the size 50 mm down to 37.5 mm was prepared, and was washed with distilled water and then oven dried at 105–110°C. A saturated solution of magnesium sulphate having density 1.292 ± 0.008 g/mL was subjected to five 48 hour immersion and drying cycles in which they were Immersed in saturated solution for 16–18 hour after drained for two hours then oven dried at 105°C for 24 hour and cooled for five hours at lab temperature. The sulphate soundness value (SSV) expressed in percentage was calculated as (Eq. 15).

$$SSV = \frac{(W_1 - W_2)}{W_1}.100 \quad (15)$$

where, $W_1$ is an initial weight of sample (kg) and $W_2$ is the weight of the sample after five cycles.

***Los Angeles abrasion test***

Los Angeles Abrasion test measures resistance of aggregates to abrasion and impact, and is an indirect test of hardness of rock. The test was carried out in LAA machine in accordance with ASTM C535 (2016). To conduct the LAA test, the Grade A test sample that constituted of 5 kg mass of aggregate of 50 mm down to 37.5 mm size and 37.5 mm down to 25 mm size was prepared, and was placed in the LAA machine along with 12 steel balls. The machine was set to revolve for 1000 revolutions. After completion of revolutions, the steel balls were taken out, and the sample was place in a tray, and was sieved at 1.7 mm sieve. The retained sample was weighed. The Los Angeles abrasion value (LAAV) was calculated using Equation 16 which measures the abrasion loss in percentage.

$$LAAV = \frac{(W_1 - W_2)}{W_1}.100 \quad (16)$$

where, $W_1$ is an initial weight of the sample and $W_2$ is the weight of the sample retained on 1.7 mm sieve.

## RESULTS AND DISCUSSIONS

Location of sampling sites and field description of samples are tabulated (Table 1), and sampling sites are indicated in Figure 2 whereas sampling horizons are shown in Figure 3. The samples and data collected from field were further analyzed for mineralogy and texture, and physical, mechanical and durability properties of ballasts.

**Geological outlines**

The Fagfog Quartzite is underlain and overlain respectively by the Kuncha Formation and the Dandagaon Phyllite, both of

**Table 1: Sample location, and description and classification of ballasts from the Fagfog Quartzite.**

| | | | Aggregate | | Physical charateristics | | | | | Petrological classification | | | | |
|---|---|---|---|---|---|---|---|---|---|---|---|---|---|---|
| S.N. | Latitude/ Longitude | Elv. (m) | Type | Source | Nominal size (mm) | Particle shape | Surface texture | Colour | Fines/ coating/ extraneous materials | Monomictic /polymictic | Name | Geological age | Description | Classific-ation |
| F1 | 27° 51 00 69 84° 51 03 23 | 466 | Crushed rock | Bed rock/ Fagfog Quartzite, uphillside, Kalu Pandey Highway | 37.5 | Very angular, bladed to prolate | Rough | White to yellowish white | None | Monomictic | Quartzite | Precambrian | Laminated, medium-grained | Crushed Quartzite |
| F2 | 27° 51 00 72 84° 51 03 04 | 464 | Crushed rock | Bed rock/ Fagfog Quartzite, uphillside, Kalu Pandey Highway | 37.5 | Very angular, bladed to prolate | Rough | Brownish white | None | Monomictic | Quartzite | Precambrian | Massive, medium-grained | Crushed Quartzite |
| F3 | 27° 51 00 20 84° 51 01 42 | 462 | Crushed rock | Bed rock/ Fagfog Quartzite, uphillside, Kalu Pandey Highway | 37.5 | Very angular, bladed to prolate | Rough | Brownish white to white | None | Monomictic | Quartzite | Precambrian | Massive, medium-grained | Crushed Quartzite |
| F4 | 27° 51 00 12 84° 51 00 69 | 461 | Crushed rock | Bed rock/ Fagfog Quartzite, uphillside, Kalu Pandey Highway | 37.5 | Very angular, bladed to prolate | Rough | Yellowish white | None | Monomictic | Quartzite | Precambrian | Massive, medium-grained | Crushed Quartzite |
| F5 | 27° 51 01 23 84° 51 06 24 | 468 | Crushed rock | Bed rock/ Fagfog Quartzite, uphillside, Kalu Pandey Highway | 37.5 | Very angular, bladed to prolate | Rough | Yellowish white | None | Monomictic | Quartzite | Precambrian | Laminated, medium-grained | Crushed Quartzite |
| F6 | 27° 51 02 51 84° 51 11 82 | 452 | Crushed rock | Bed rock/ Fagfog Quartzite, uphillside, Kalu Pandey Highway | 37.5 | Very angular, bladed to prolate | Rough | Brownish white | None | Monomictic | Quartzite | Precambrian | Massive, medium-grained | Crushed Quartzite |
| F7 | 27°51'03.63" 84°1'09.51" | 452 | Crushed rock | Bed rock/ Fagfog Quartzite, uphillside, Kalu Pandey Highway | 37.5 | Very angular, bladed to prolate | Rough | Brownish white | None | Monomictic | Quartzite | Precambrian | Massive, medium-grained | Crushed Quartzite |
| F8 | 27° 51 01 95 84° 51 07 40 | 453 | Crushed rock | Bed rock/ Fagfog Quartzite, uphillside, Kalu Pandey Highway | 37.5 | Very angular, bladed to prolate | Rough | White | None | Monomictic | Quartzite | Precambrian | Massive, medium-grained | Crushed Quartzite |
| F9 | 27°51'02.05" 84°51'31.37" | 441 | Crushed rock | Bed rock/ Fagfog Quartzite, uphillside, Kalu Pandey Highway | 37.5 | Very angular, bladed to prolate | Rough | White to brownish white | None | Monomictic | Quartzite | Precambrian | Massive, medium-grained | Crushed Quartzite |
| F10 | 27°51´07.96" 84°51´2270" | 424 | Crushed rock | Bed rock/ Fagfog Quartzite, uphillside, Kalu Pandey Highway | 37.5 | Very angular, bladed to prolate | Rough | White | None | Monomictic | Quartzite | Precambrian | Massive, medium-grained | Crushed Quartzite |
| F11 | 27° 51´06. 81" 84° 51´22.19" | 423 | Crushed rock | Bed rock/ Fagfog Quartzite, uphillside, Kalu Pandey Highway | 37.5 | Very angular, bladed to prolate | Rough | White | None | Monomictic | Quartzite | Precambrian | Massive, medium-grained | Crushed Quartzite |
| F12 | 27° 51´06. 47" 84° 51´21.82" | 422 | Crushed rock | Bed rock/ Fagfog Quartzite, uphillside, Kalu Pandey Highway | 37.5 | Very angular, bladed to prolate | Rough | Brownish white | None | Monomictic | Quartzite | Precambrian | Massive, medium-grained | Crushed Quartzite |
| F13 | 27° 51´06.55" 84° 51´22.05" | 422 | Crushed rock | Bed rock/ Fagfog Quartzite, uphillside, Kalu Pandey Highway | 37.5 | Very angular, bladed to prolate | Rough | White | None | Monomictic | Quartzite | Precambrian | Massive, medium-grained | Crushed Quartzite |
| F14 | 27°21'06.02" 84°51'21.38" | 422 | Crushed rock | Bed rock/ Fagfog Quartzite, uphillside, Kalu Pandey Highway | 37.5 | Very angular, bladed to prolate | Rough | Brownish white | None | Monomictic | Quartzite | Precambrian | Massive, medium-grained | Crushed Quartzite |
| F15 | 27°51 04 47 84°51 20 10 | 427 | Crushed rock | Bed rock/ Fagfog Quartzite, uphillside, Kalu Pandey Highway | 37.5 | Very angular, bladed to prolate | Rough | White | None | Monomictic | Quartzite | Precambrian | Laminated, medium-grained | Crushed Quartzite |

these units are distinct from the Fagfog Quartzite unit as they contain phyllite which are distinct from the white quartzites of the Fagfog Quartzite. All those three units belong to the Lower Nawakot Group of the Nawakot Complex. Beds are overturned and roughly extend NW-SE. All the quartzites are medium-grained, brownish or yellowish white to white (Table 1). Most of the quartzites show massive structure and few of them from the lower and the upper parts of the formation are of laminated structure (Fig. 3).

**Description and classification of samples**

The ballasts were described and classified considering three attributes, i.e. aggregate type, physical and petrological characteristics (Table 1). All the quartzite samples are from the bedrocks of the Fagfog Quartzite. Almost all the samples have nominal size 37.5 mm, and show very angular, bladed to prolate shapes, rough surface texture, and white to yellowish or brownish white colours. Coating and extraneous materials are absent. These samples are medium-grained monomictic quartzite of Precambrian Age (Stöcklin and Bhattarai, 1980). All the samples are classified as crushed quartzites because samples come from crushing of the large fragments obtained from the bedrocks.

**Texture, fabric, microstructure and mineral composition**

Quartzites have grain size ranging from 0.25 mm to 1.3 mm showing that they belong to medium-grained category. In each sample, the grain size range is quite wide and are inequigranular. Grains are subequant to equant, and are subrounded to rounded (in F1 and F2), subangular to subrounded (in F3, F4, F5, F8 and F13), very angular to subangular (F8 and F9), angular to subangular (6, 11 and 14), and angular to subrounded (10, 12 and 15). Contacts among grains are long to sutured. Grain boundaries are irregular and except for F13, F14 and F15, the rest of the grains show undulosity and nearly preferredly oriented grains.

Almost all the quartzite samples exhibit dynamic recrystallization (Table 2). Three distinct microtextures of quartz under dynamic recrystallization are bulging (BLG) recrystallization (low T), subgrain rotation (SGR) recrystallization (intermediate T), and grain boundary migration (GBM) recrystallization (high T) (Stipp et al., 2002). Samples show mortar texture, in which porphyroclasts are surrounded by recrystallized subgrains (Howard, 2005). Only some of the samples preserve bulging grain (BLG) recrystallization (as in F5, F6, F8, F10, F14 and F15; Fig. 4), whereas subgrain rotation (SGR) microstructure is distinct in all the samples (Table 2, Figs. 4, 5, 6).

The proportion of porphyroclast quartz and subgrain quartz are found to be more or less subequal in quartzites showing SGR and lacking BLG (Fig. 4). But the quartzites undergoing both BLG and SGR recrystallization show exceeding porphyrocasts over subgrains, e.g., QP 70 to QS 21 where total quartz QT is 91 (Table 2; Figs. 5, 6). The QT ranges between 89% and 93% in the model composition. Chert, biotite, tourmaline, sericite and ferruginous material represent minor constituents and vary in total from 6 to 11% of the model composition. Based on mortar texture, SGR recrystallization microstructure and presence of biotite, the quartzites have experienced low-grade metamorphism with intermediate temperature. The fabric and microstructure, therefore slightly differ among quartzites whereas total content of quartz remains within narrow range.

**Shape indices of Fagfog Quarzite**

Shape indices are a geometrically derived value to distinguish the morphology of individual particles. Flakiness and Elongation Indices were determined and listed for quartzite ballasts of each of the samples (Table 3).

Flakiness is the percentage by weight of particles, whose thickness is less than 0.6 times the average size of the particles between passing and retained sieves. Flakiness Index ranges between 0.92% (in F2) and 8.80% (in F13). Flakiness index remains approximately below 9% and since quartzites are strongly interlocked, flakiness is not influenced by structure.

Elongation Index is the percentage by weight of particles whose length is greater than 1.8 times the average size of the particles between passing and retained sieves. Elongation Index varies between 26.33% (F11) and 56.68% (in F2). It shows that the tendency to break quartzite in to ballast particles seems somewhat elongated. There is no distinct bearing of grain size on shape, as all the quartzites belong to medium-grained category. Except F2, F3 and F6, the rest of the samples have Elongation Index below 40% and are suitable according to UK Railway Standards (BS EN13450, 2013).

**Physical properties**

***Specific gravity, density and water absorption***

The specific gravity also known as relative density ranges from 2.38 (F1 sample) to 2.70 (F12 sample) (Table 4). Variation of specific gravity and density both in oven-dried basis, is limited to narrow range and particles fall in to normal weight aggregates. Density does not rely on quartz content in this study which is opposed to the result of increasing density with increased amount of quartz obtained by Gupta and Sharma (2012). The quartzites they studied were of medium- to coarse-grained, sillimanite grade with highly preferred orientation of grains. Water absorption determines the ability of aggregate to absorb water in the moist environment and does indicate connectivity of voids from the surface inwards of the particles. Water absorption ranges from 0 (as in F3 and F4) to 2.50% (as in F12) (Table 4). Four samples show water absorption of more than 1%. The sample F12 has the highest water absorption despite of high apparent density. This can be because of presence of connected pores around particles.

***Bulk density***

Bulk density includes both void spaces among aggregate particles and the density contributed by particles. Bulk density ranges from 1203.62 kg/m$^3$ (sample F13) to 1386.88 kg/m$^3$ (sample F6) (Table 4). All the ballast samples possess bulk density within the specified value of bulk density of 1120 kg/m$^3$ by AREMA (2010).

**Strength properties**

***Point load strength index***

Point load strength index (PLSI) determines the strength index value at the given point. It ranges from 2.40 to 11.45 MPa (Table 5). Samples F7 and F13 respectively possess the least and the highest indices. The corresponding uniaxial compressive strength (UCS) derived from empirical relation ranges respectively from 39 to 302 MPa. The quartzite samples are moderately strong to extremely strong and majority are

**Table 2: Results of texture, fabric, microstructure and composition of the Fagfog Quartzite.**

| Sample No. | Texture | | Fabric | | | **Microstructure | | Undulosity | ***Composition | | | | | | | | |
|---|---|---|---|---|---|---|---|---|---|---|---|---|---|---|---|---|---|
| | Grain size | *Shape | Grain contact | Grain boundary | Orientation | BLG | SGR | | QP | QS | QT | Chr | Bi | To | Ser | Fer | Total |
| Fg 1 | often 0.31–0.6, up to 1 mm | SE to E, SR–R | long to sutured | irregular | nearly preferred | | SGR | undulose | 50 | 41 | 91 | | 2 | 1 | 5 | 1 | 100 |
| Fg 2 | often 0.31–0.6, up to 1 mm | SE to E, SR–R | long to sutured | irregular | nearly preferred | | SGR | undulose | 51 | 40 | 91 | | 2 | 1 | 3 | 3 | 100 |
| Fg 3 | often 0.31–0.6, upto 2 mm | SE to E, SA–SR | long to sutured | irregular | nearly preferred | | SGR | undulose | 55 | 39 | 94 | 2 | 1 | | 2 | 1 | 100 |
| Fg 4 | often 0.31–0.6, upto 1.2 mm | SE to E, SA–SR | long to sutured | irregular | nearly preferred | | SGR | undulose | 45 | 47 | 92 | | 1 | 1 | 5 | 1 | 100 |
| Fg 5 | often 0.41–0.6, upto 1.2 mm | SE, SA–SR | sutured | irregular | nearly preferred | BLG | minor SGR | undulose | 70 | 21 | 91 | | 2 | 1 | 5 | 1 | 100 |
| Fg 6 | often 0.31–0.5, upto 0.8 mm | SE to E, A–SA | long to sutured | irregular | nearly preferred | BLG | minor SGR | undulose | 65 | 25 | 90 | | 2 | 1 | 6 | 1 | 100 |
| Fg 7 | often 0.31–0.6, upto 1.2 mm | SE to E, VA–SA | long to sutured | irregular | nearly preferred | | SGR | undulose | 55 | 38 | 93 | | 1 | 1 | 4 | 1 | 100 |
| Fg 8 | often 0.41–0.6, upto 1.0 mm | SE to E, SA–SR | long to sutured | irregular | nearly preferred | minor BLG | SGR | undulose | 40 | 50 | 90 | 2 | 1 | 1 | 5 | 1 | 100 |
| Fg 9 | often 0.41–0.6, upto 1.0 mm | SE to E, VA–SA | long to sutured | irregular | nearly preferred | | SGR | undulose | 35 | 55 | 90 | 1 | 1 | 1 | 4 | 3 | 100 |
| Fg 10 | often 0.61–0.8, upto 1.0 mm | SE to E, A–SR | long to sutured | irregular | nearly preferred | BLG | SGR | undulose | 70 | 22 | 92 | 3 | 1 | | 4 | | 100 |
| Fg 11 | often 0.21–0.5, upto 0.5 mm | SE to E, A–SA | long to sutured | irregular | nearly preferred | | SGR | undulose | 30 | 62 | 92 | 1 | 1 | 1 | 5 | | 100 |
| Fg 12 | often 0.41–0.6, upto 1.0 mm | SE to E, A–SR | long to sutured | irregular | nearly preferred | | SGR | undulose | 30 | 61 | 91 | | 3 | 1 | 5 | | 100 |
| Fg 13 | often 0.61–0.7, upto 1.2 mm | SE to E, SA–SR | long to sutured | irregular | less preferred | | SGR | undulose | 65 | 26 | 91 | | 1 | 1 | 5 | 2 | 100 |
| Fg 14 | often 0.41–0.8, upto 1.3 mm | SE to E, A–SA | long to sutured | irregular | less preferred | minor BLG | SGR | undulose | 60 | 29 | 89 | 1 | 1 | 1 | 6 | 2 | 100 |
| Fg 15 | often 0.41–0.6, upto 0.8 mm | SE to E, A–SR | long to sutured | irregular | less preferred | minor BLG | SGR | undulose | 70 | 21 | 91 | | 1 | 1 | 6 | 1 | 100 |

*Shape: SE=subequant; E=elongate; R=rounded; SR=subrounded; SA=subangular; A=angular; VA=very angular

**Microstucture: BLG=buldging grain recrystallization; SGR=sediment grain rotation

***Composition: QP=quartz porphyroclast; QS=quartz subgrain; QT=quartz total; Chr=chert; Bi = biotite; To=tourmaline; Ser=sericite; Fer=ferruginous material

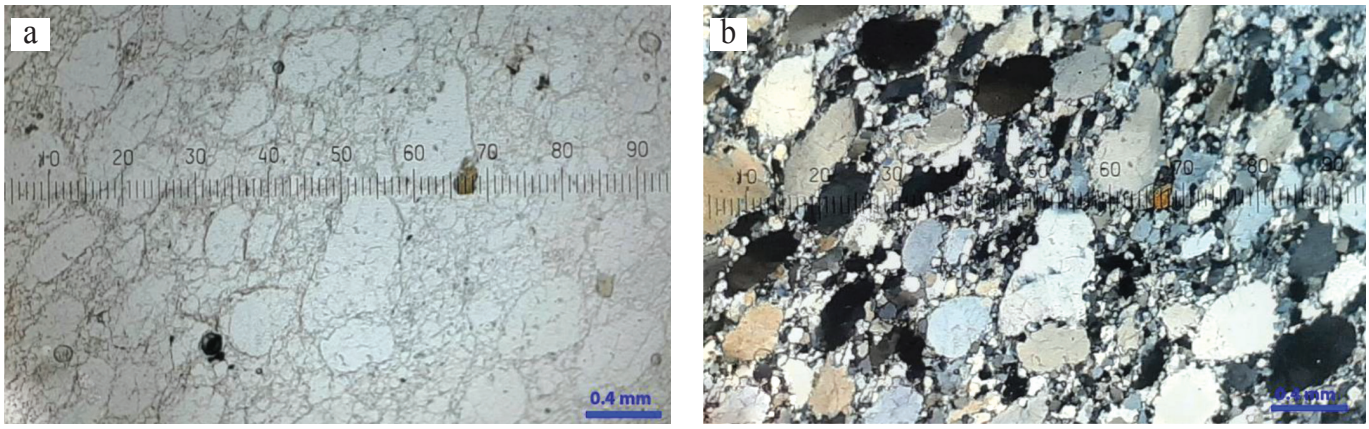


**Fig. 4: Photomicrographs of quartzite (F5) of the Fagfog Quartzite from uphill side of the Kalu Pande Highway, Bungchug area, Dhanding District. (a) Under plane polarized light, (b) under cross polarized light showing porphyroclasts and subgrains of mostly BGR with minor SGR recrystallization.**

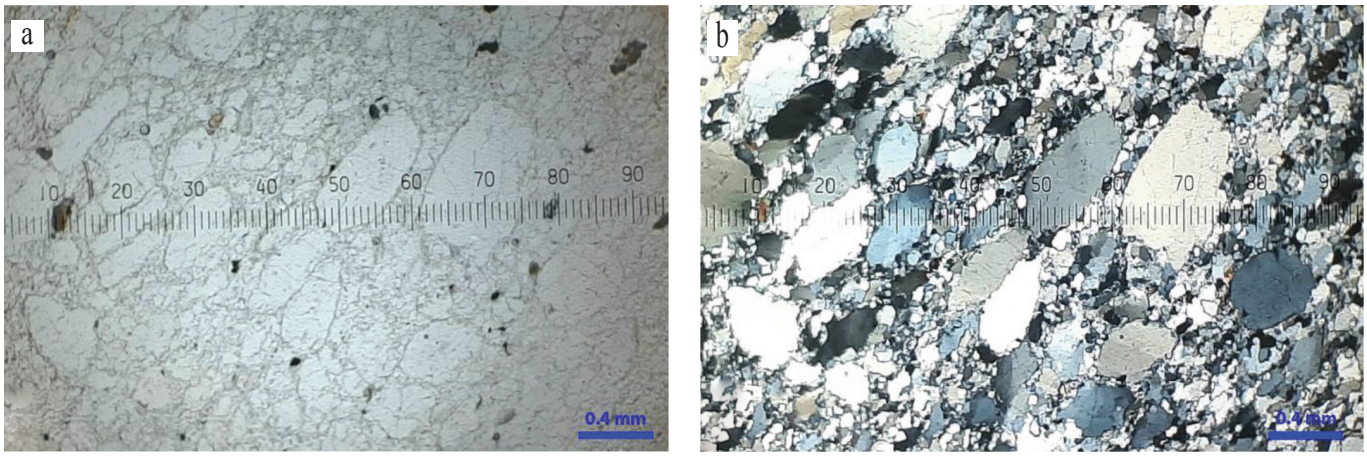


**Fig. 5: Photomicrographs of quartzite (F1) of the Fagfog Quartzite from uphill side of the Kalu Pande Highway, Bungchug area, Dhanding District. (a) Under plane polarized light, (b) under Cross polarized light showing porphyroclasts and subgrains of SGR recrystallization.**

**Table 3: Flakiness and elongation indices of ballasts from the Fagfog Quartzite.**

| Sample No. | Passing through sieve | Retained Sieve | Thickness Gauge size (average sieves x 0.6) | Initial weight of ballast retained | Weight passing through the thickness gauge | Flakiness Index, FI | FI of total | Length gauge size (average sieves x 1.8) | Initial weight of ballast retained | Weight retained on the length gauge | Elongation Index, EI | EI of total |
|---|---|---|---|---|---|---|---|---|---|---|---|---|
| | mm | mm | mm | kg | kg | % | % | mm | kg | kg | % | % |
| F1 | 50.00 | 37.50 | 26.30 | 10.130 | 0.490 | 4.84 | 5.63 | 78.70 | 10.130 | 2.485 | 24.53 | 33.34 |
| | 37.50 | 25.00 | 18.75 | 5.045 | 0.365 | 7.23 | | 56.30 | 5.045 | 2.575 | 51.04 | |
| F2 | 50.00 | 37.50 | 26.30 | 10.075 | 0.090 | 0.89 | 0.92 | 78.70 | 10.075 | 4.730 | 46.95 | 56.68 |
| | 37.50 | 25.00 | 18.75 | 5.150 | 0.050 | 0.97 | | 56.30 | 5.150 | 3.900 | 75.73 | |
| F3 | 50.00 | 37.50 | 26.30 | 10.085 | 0.145 | 1.44 | 2.18 | 78.70 | 10.085 | 4.475 | 44.37 | 50.96 |
| | 37.50 | 25.00 | 18.75 | 5.045 | 0.185 | 3.67 | | 56.30 | 5.045 | 3.235 | 64.12 | |
| F4 | 50.00 | 37.50 | 26.30 | 10.105 | 0.735 | 7.27 | 6.87 | 78.70 | 10.105 | 2.105 | 20.83 | 38.50 |
| | 37.50 | 25.00 | 18.75 | 5.025 | 0.305 | 6.07 | | 56.30 | 5.025 | 3.720 | 74.03 | |
| F5 | 50.00 | 37.50 | 26.30 | 10.170 | 0.390 | 3.83 | 3.42 | 78.70 | 10.170 | 2.975 | 29.25 | 35.67 |
| | 37.50 | 25.00 | 18.75 | 5.335 | 0.140 | 2.62 | | 56.30 | 5.335 | 2.555 | 47.89 | |
| F6 | 50.00 | 37.50 | 26.30 | 10.197 | 0.285 | 2.79 | 4.56 | 78.70 | 10.197 | 4.635 | 45.45 | 51.00 |
| | 37.50 | 25.00 | 18.75 | 5.145 | 0.415 | 8.07 | | 56.30 | 5.145 | 3.190 | 62.00 | |
| F7 | 50.00 | 37.50 | 26.30 | 10.430 | 0.415 | 3.98 | 4.04 | 78.70 | 10.430 | 2.785 | 26.70 | 40.95 |
| | 37.50 | 25.00 | 18.75 | 5.040 | 0.210 | 4.17 | | 56.30 | 5.040 | 3.550 | 70.44 | |
| F8 | 50.00 | 37.50 | 26.30 | 10.055 | 0.880 | 8.75 | 7.77 | 78.70 | 10.055 | 3.140 | 31.23 | 35.85 |
| | 37.50 | 25.00 | 18.75 | 5.135 | 0.300 | 5.84 | | 56.30 | 5.135 | 2.305 | 44.89 | |
| F9 | 50.00 | 37.50 | 26.30 | 10.055 | 0.390 | 3.88 | 7.41 | 78.70 | 10.055 | 4.575 | 45.50 | 46.41 |
| | 37.50 | 25.00 | 18.75 | 5.135 | 0.735 | 14.31 | | 56.30 | 5.135 | 2.475 | 48.20 | |
| F10 | 50.00 | 37.50 | 26.30 | 10.505 | 0.177 | 1.68 | 2.83 | 78.70 | 10.505 | 2.250 | 21.42 | 31.94 |
| | 37.50 | 25.00 | 18.75 | 5.290 | 0.270 | 5.10 | | 56.30 | 5.290 | 2.795 | 52.84 | |
| F11 | 50.00 | 37.50 | 26.30 | 9.740 | 0.655 | 6.72 | 6.41 | 78.70 | 9.740 | 1.775 | 18.22 | 26.33 |
| | 37.50 | 25.00 | 18.75 | 5.150 | 0.300 | 5.83 | | 56.30 | 5.150 | 2.145 | 41.65 | |
| F12 | 50.00 | 37.50 | 26.30 | 10.105 | 0.765 | 7.57 | 8.11 | 78.70 | 10.105 | 3.125 | 30.93 | 34.70 |
| | 37.50 | 25.00 | 18.75 | 5.055 | 0.47 | 9.20 | | 56.30 | 5.055 | 2.135 | 42.24 | |
| F13 | 50.00 | 37.50 | 26.30 | 9.935 | 0.98 | 9.81 | 8.80 | 78.70 | 9.935 | 1.045 | 10.52 | 28.85 |
| | 37.50 | 25.00 | 18.75 | 5.350 | 0.37 | 6.92 | | 56.30 | 5.350 | 3.365 | 62.90 | |
| F14 | 50.00 | 37.50 | 26.30 | 10.400 | 0.78 | 7.50 | 6.54 | 78.70 | 10.400 | 2.455 | 23.61 | 36.77 |
| | 37.50 | 25.00 | 18.75 | 5.130 | 0.24 | 4.58 | | 56.30 | 5.130 | 3.255 | 63.45 | |
| F15 | 50.00 | 37.50 | 26.30 | 10.275 | 0.19 | 1.85 | 2.07 | 78.70 | 10.275 | 2.205 | 21.46 | 33.34 |
| | 37.50 | 25.00 | 18.75 | 5.170 | 0.13 | 2.51 | | 56.30 | 5.170 | 2.945 | 56.96 | |

**Table 4: Density, specific gravity, water absorption and bulk density of quartzites from the Fagfog Quartzite.**

| Sample No. | Mass of oven-dry sample in air (kg) | Mass of saturated surface dry (SSD) wt. in air (kg) | Mass of saturated sample immersed in water (kg) | Specific gravity (Oven-dry) | Density (Oven-dry), (kg/m$^3$) | Water absorption, (%) | Mass of ballast (kg) | Volume of bucket (m$^3$) | Bulk density (kg/m$^3$) |
|---|---|---|---|---|---|---|---|---|---|
| | A | B | C | {A/(B-C)} | 997.5 {A/(B-C)} | {(B-A)/A}100 | | | |
| F1 | 2.035 | 2.070 | 1.201 | 2.34 | 2335.92 | 1.72 | 2.720 | 0.00221 | 1230.77 |
| F2 | 2.140 | 2.155 | 1.330 | 2.59 | 2587.45 | 0.70 | 2.945 | 0.00221 | 1332.58 |
| F3 | 2.065 | 2.065 | 1.220 | 2.44 | 2437.68 | 0.00 | 3.033 | 0.00221 | 1372.62 |
| F4 | 2.105 | 2.105 | 1.310 | 2.65 | 2641.18 | 0.00 | 2.846 | 0.00221 | 1287.71 |
| F5 | 2.050 | 2.060 | 1.260 | 2.56 | 2556.09 | 0.49 | 3.053 | 0.00221 | 1381.29 |
| F6 | 2.007 | 2.030 | 1.245 | 2.56 | 2550.30 | 1.15 | 3.065 | 0.00221 | 1386.88 |
| F7 | 2.040 | 2.040 | 1.235 | 2.53 | 2527.83 | 0.00 | 2.965 | 0.00221 | 1341.63 |
| F8 | 2.075 | 2.085 | 1.260 | 2.52 | 2508.86 | 0.48 | 3.005 | 0.00221 | 1359.52 |
| F9 | 2.025 | 2.040 | 1.255 | 2.58 | 2573.17 | 0.74 | 2.815 | 0.00221 | 1273.88 |
| F10 | 2.080 | 2.125 | 1.290 | 2.49 | 2484.79 | 2.16 | 2.964 | 0.00221 | 1341.35 |
| F11 | 2.035 | 2.055 | 1.245 | 2.51 | 2506.06 | 0.98 | 2.850 | 0.00221 | 1289.82 |
| F12 | 2.000 | 2.050 | 1.290 | 2.63 | 2625.00 | 2.50 | 2.860 | 0.00221 | 1294.12 |
| F13 | 2.050 | 2.060 | 1.235 | 2.48 | 2478.64 | 0.49 | 2.660 | 0.00221 | 1203.62 |
| F14 | 2.050 | 2.070 | 1.270 | 2.56 | 2556.09 | 0.98 | 2.705 | 0.00221 | 1223.98 |
| F15 | 2.025 | 2.040 | 1.235 | 2.52 | 2509.24 | 0.74 | 2.835 | 0.00221 | 1282.81 |

strong to very strong according to the ISRM (1979, 1981). Considering the amount of load required to break ballast as per AREMA (2010), the very strong and extremely strong ballast samples seem to be suitable for railway ballasts.

### *Aggregate impact value*

The aggregate impact value is a measure of resistance to sudden impact, which may differ from its resistance to gradually applied compressive load. In short it measures the toughness of the aggregate. The result shows that sample F13 possesses the lowest AIV of 14.85% whereas sample F15 possesses the highest AIV of 21.57% (Table 6). AIV of the Fagfog Quartzite samples exhibit good resistance to impact as AIV lies within specified limits (20–22%) of UK Railway (EN13450, 2013) and Indian Railway (IRS-GE-1, 2004; IRS-GE-1, 2016).

### *Aggregate Crushing Value*

The aggregate crushing value (ACV) provides relative measure of the resistance of an aggregate to crush under a gradually applied compressive load. The result shows that the ACV ranges between 15.51% (as of sample F5) and 29.70% (as of sample F9) (Table 5). ACV below 22% is suitable for aggregates to be used for ballasts according to UK Railway (EN13450, 2013). The Fagfog Quartzite is therefore suitable for the railway ballasts because the majority of the samples give ACV <22%.

## Durability

Three durability attributes, i.e., slake durability index ($I_{d2}$), sulphate soundness value (SSV) and Los Angeles Abrasion value (LAAV) have been determined to assess durability of quartzite.

### *Slake durability index*

Slake durability index is a weathering test that determines the resistance to slaking under cyclic wetting and drying. Five-cycle slake durability test was conducted instead of standard two-cycle test in order to obtain deterioration character of rocks under more cycles. The two-cycle slake durability index ($I_{d2}$) varies between 96.94 and 100% (Table 6). Sample F3, F6 and F7 are of high durability and the rest are of very high durability against slaking. The least and the maximum slake durability index up to the fifth cycle, $I_{d5}$ are respectively 95.1% and 99.11%. There has occurred 1 to 2% diminish in index between the second and the fifth cycles (Table 6; Fig. 7). Samples F1, F2, F3, F4, F5, F10, F12 and F13 undergo type I deterioration and the remaining samples undergo type II deterioration (Fig. 8). F1, F2, F3, F4, F5, F7, F9, F10, F11, F14 and F15 all show type II deterioration after fifth cycle. Among these, F7, F9, F11, F14 and F15, which did not deteriorate showing type II at the second cycle, have deteriorated as type II under more repeated cycles of test. It shows that though

**Table 5: Results of point-load strength index, aggregate impact value (AIV) and aggregate crushing value (ACV) of ballast from the Fagfog Quartzite.**

| Sample No. | $W_{avg}$, mm | $D_{avg}$, mm | $De^2$ =4WD/p, $mm^2$ | Load, P, KN | $I_s$ = P/ $De^2$,Mpa | F = (De/50)^^0.45 | $I_{s(50)}$ = $I_s$. F, Mpa | Average $I_{s(50)}$, Mpa | UCS=24*$I_{s(50)}$, Mpa | *Remarks | AIV (%) | ACV (%) |
|---|---|---|---|---|---|---|---|---|---|---|---|---|
| F1 | 31.50 | 14.60 | 585.49 | 6.00 | 10.25 | 0.72 | 7.39 | 6.82 | 177 | Very strong | 16.67 | 21.73 |
| | 34.20 | 13.20 | 574.72 | 5.00 | 8.70 | 0.72 | 6.25 | | | | | |
| F2 | 48.35 | 39.70 | 2443.66 | 14.00 | 5.73 | 0.99 | 5.70 | 4.93 | 137 | Very strong | 18.81 | 21.46 |
| | 47.90 | 20.10 | 1225.70 | 6.00 | 4.90 | 0.85 | 4.17 | | | | | |
| F3 | 44.05 | 28.90 | 1620.68 | 7.00 | 4.32 | 0.91 | 3.92 | 4.70 | 94 | Strong | 18.81 | 20.03 |
| | 49.40 | 28.20 | 1773.49 | 10.50 | 5.92 | 0.93 | 5.48 | | | | | |
| F4 | 53.50 | 29.95 | 2039.88 | 5.50 | 2.70 | 0.96 | 2.58 | 3.07 | 62 | Strong | 17.48 | 21.63 |
| | 50.25 | 31.25 | 1999.12 | 7.50 | 3.75 | 0.95 | 3.57 | | | | | |
| F5 | 40.90 | 36.60 | 1905.72 | 18.00 | 9.45 | 0.94 | 8.89 | 8.15 | 213 | Very strong | 22.77 | 15.51 |
| | 45.45 | 30.10 | 1741.62 | 14.00 | 8.04 | 0.92 | 7.41 | | | | | |
| F6 | 48.00 | 33.35 | 2037.94 | 6.00 | 2.94 | 0.96 | 2.81 | 4.52 | 67 | Strong | 15.00 | 16.54 |
| | 58.50 | 32.05 | 2386.92 | 15.00 | 6.28 | 0.99 | 6.22 | | | | | |
| F7 | 49.85 | 45.00 | 2855.82 | 4.50 | 1.58 | 1.03 | 1.62 | 2.40 | 39 | Medium strong | 17.82 | 20.30 |
| | 65.60 | 30.15 | 2517.94 | 8.00 | 3.18 | 1.00 | 3.18 | | | | | |
| F8 | 49.75 | 26.35 | 1668.89 | 6.50 | 3.89 | 0.91 | 3.56 | 4.18 | 85 | Strong | 16.83 | 22.57 |
| | 52.05 | 41.80 | 2769.82 | 13.00 | 4.69 | 1.02 | 4.80 | | | | | |
| F9 | 45.75 | 36.95 | 2152.08 | 11.00 | 5.11 | 0.97 | 4.94 | 6.02 | 119 | Very strong | 19.61 | 29.70 |
| | 49.90 | 38.65 | 2455.30 | 17.50 | 7.13 | 1.00 | 7.10 | | | | | |
| F10 | 60.00 | 33.55 | 2562.70 | 8.50 | 3.32 | 1.01 | 3.34 | 3.48 | 80 | Strong | 18.00 | 21.87 |
| | 52.20 | 24.50 | 1628.13 | 6.50 | 3.99 | 0.91 | 3.63 | | | | | |
| F11 | 49.45 | 39.35 | 2477.22 | 16.00 | 6.46 | 1.00 | 6.45 | 6.66 | 155 | Very strong | 17.82 | 20.70 |
| | 48.20 | 43.25 | 2653.91 | 18.00 | 6.78 | 1.01 | 6.87 | | | | | |
| F12 | 41.65 | 33.50 | 1776.29 | 11.50 | 6.47 | 0.93 | 5.99 | 4.23 | 144 | Very strong | 17.00 | 22.17 |
| | 55.55 | 45.60 | 3224.80 | 7.50 | 2.33 | 1.06 | 2.46 | | | | | |
| F13 | 40.40 | 33.30 | 1712.69 | 23.50 | 13.72 | 0.92 | 12.60 | 11.55 | 302 | Extremely strong | 14.85 | 20.00 |
| | 43.70 | 29.60 | 1646.75 | 19.00 | 11.54 | 0.91 | 10.50 | | | | | |
| F14 | 59.80 | 58.95 | 4487.85 | 14.00 | 3.12 | 1.14 | 3.56 | 2.93 | 85 | Strong | 18.00 | 20.70 |
| | 72.50 | 28.75 | 2653.56 | 6.00 | 2.26 | 1.01 | 2.29 | | | | | |
| F15 | 41.75 | 35.00 | 1860.28 | 12.00 | 6.45 | 0.94 | 6.04 | 5.42 | 145 | Very strong | 21.57 | 19.93 |
| | 38.40 | 35.15 | 1718.35 | 9.00 | 5.24 | 0.92 | 4.81 | | | | | |

*ISRM (1981): 0.25–1 MPa= extremely weak; 1–5.0 MPa= very weak; 5.0–25 MPa = weak; 25–50 MPa= medium strong rock; 50–100 MPa= strong; 100–250 MPa= very strong; >250 MPa extremely strong

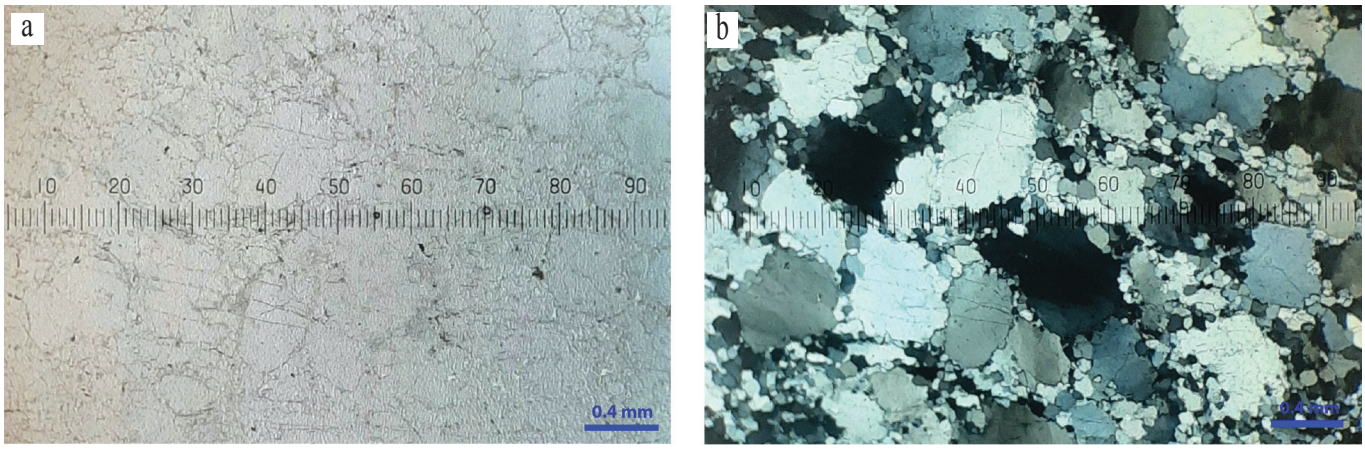


**Fig. 6: Photomicrographs of quartzite (F10) of the Fagfog Quartzite from uphill side of the Kalu Pande Highway, Bungchug area, Dhanding District. (a) Under plane polarized light and (b) under cross polarized light showing porphyroclasts and subgrains of SGR recrystallization.**

**Table 6: Results of slake durability Index of quartzites from the Fagfog Quartzite.**

| Sample No. | Initial wt. (g) | Initial oven-dry wt. before the 1st cycle (g) | Moisture content (%) | $I_{d1}$ (%) | *$I_{d2}$ (%) | $I_{d3}$ (%) | $I_{d4}$ (%) | $I_{d5}$ (%) | Durability category based on $I_{d2}$ | Deterioration type after 2nd cycle | Deterioration trend upto 5th cycle |
|---|---|---|---|---|---|---|---|---|---|---|---|
| F1 | 565 | 565 | 0.00 | 98.23 | 98.23 | 98.23 | 98.23 | 98.23 | VHD | I | no deterioration, constant trend |
| F2 | 505 | 505 | 0.00 | 99.01 | 99.01 | 99.01 | 99.01 | 99.01 | VHD | I | no deterioration, constant trend |
| F3 | 530 | 530 | 0.00 | 100.00 | 97.17 | 97.17 | 97.17 | 97.17 | HD | I | deterioration-constant after 2nd-cycle |
| F4 | 570 | 565 | 0.88 | 99.12 | 99.12 | 99.12 | 98.23 | 98.23 | VHD | I | constant-deterioration-constant |
| F5 | 530 | 525 | 0.94 | 100.00 | 100.00 | 99.05 | 98.10 | 98.10 | VHD | I | constant-deterioration-constant |
| F6 | 490 | 490 | 0.00 | 97.96 | 96.94 | 96.94 | 95.92 | 95.92 | HD | II | deterioration-constant-deterioration-constant |
| F7 | 520 | 520 | 0.00 | 98.08 | 97.12 | 97.12 | 97.12 | 95.19 | HD | II | deterioration-constant-deterioration |
| F8 | 555 | 555 | 0.00 | 99.10 | 98.20 | 98.20 | 95.50 | 95.50 | VHD | II | deterioration-constant-deterioration-constant |
| F9 | 560 | 560 | 0.00 | 99.11 | 99.11 | 99.11 | 99.11 | 99.11 | VHD | II | no deterioration, constant trend |
| F10 | 515 | 510 | 0.97 | 100.00 | 100.00 | 100.00 | 100.00 | 99.02 | VHD | I | constant-deterioration after 4th-cycle |
| F11 | 490 | 490 | 0.00 | 98.98 | 98.98 | 98.98 | 98.98 | 98.98 | VHD | II | no deterioration, constant trend |
| F12 | 470 | 470 | 0.00 | 100.00 | 98.94 | 98.94 | 98.94 | 98.94 | VHD | I | deterioration-constant after 2nd-cycle |
| F13 | 530 | 530 | 0.00 | 100.00 | 99.06 | 99.06 | 99.06 | 99.06 | VHD | I | deterioration-constant after 2nd-cycle |
| F14 | 495 | 490 | 1.01 | 100.00 | 100.00 | 98.98 | 98.98 | 98.98 | VHD | II | constant-deterioration-constant |
| F15 | 520 | 520 | 0.00 | 99.04 | 99.04 | 99.04 | 99.04 | 99.04 | VHD | II | no deterioration, constant trend |

* Gambles Slake Durability Classification (Goodman, 1980): $I_{2nd}$: >98% very high durability; 95–98% high durability; 85–95 medium high durability; 60–85 medium durability; 30–60 low durability; <30 very low durability

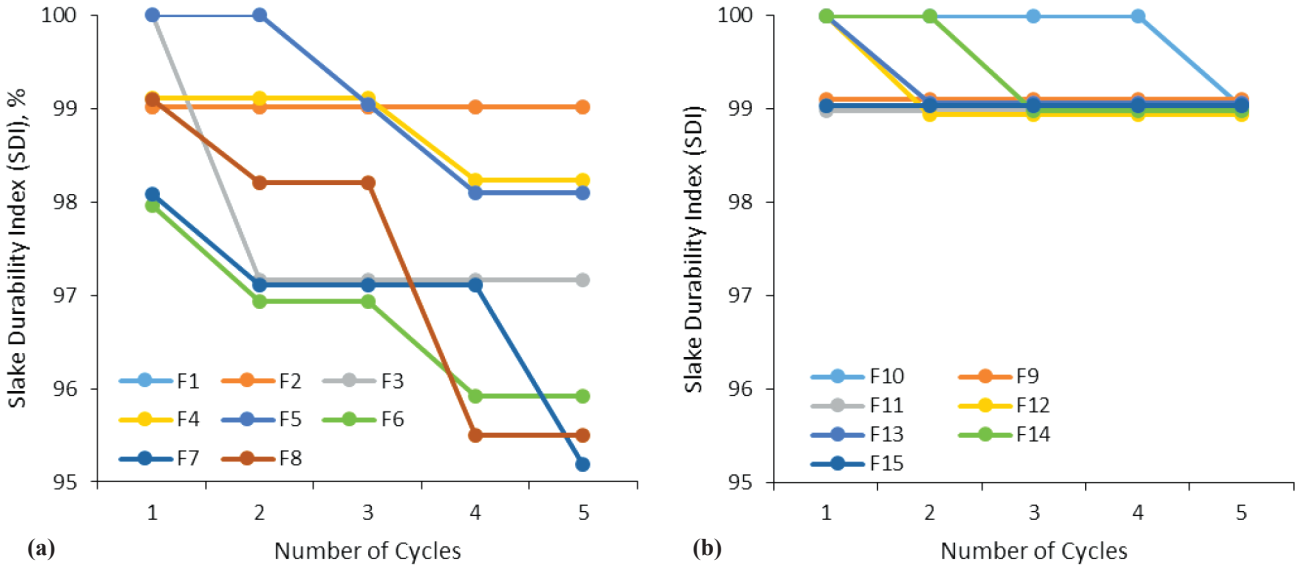


**Fig. 7: Slaking behavior of quartzites from the Fagfog Quartzite under five-cycle slake durability test. (a) Quartzites samples F1 to F8, (b) quartzites samples F9 to F15.**


**Fig. 8: Deterioration at 2nd and 5th cycles of slake durability test of quartzites from the Fagfog Quartzite. Samples F1, F2, F3, F4, F5, F10, F12 and F13 undergo type I deterioration and the remaining samples undergo type II deterioration.**

samples survive fragmentation under second-cycle test are prone to fragmentation under more cycles.

Slake durability has very weak correlation with shape indices and dry density of quartzite (Fig. 9). Slake durability index of quartzite in present study ($I_{d2}$) also does not have good correlation with water absorption, but other researchers have obtained good inverse correlation between slake durability index and water absorption (Fereidooni and Khajevand, 2017). Slake durability index also has very weak correlation with $I_{s(50)}$, AIV and ACV (Fig. 10), and thus is independent of strength parameters.

***Sulphate soundness value***

Sulphate soundness is a cyclical test that evaluates aggregates for durability and resistance to degradation from weather cycles. Magnesium sulphate soundness value (SSV) ranges from 0.20% (as in F1) to 4.59% (as in F5) (Table 7). SSV has very weak correlation with shape indices and dry density of quartzites (Fig. 9). SSV has weak correlations with $Is_{(50)}$ and AIV, but very weak correlation with ACV.

Ten samples show SSV between 1% and 5% whereas five samples remain below 1%. The obtained SSV are remarkably low, hence the quartzites reflect appreciable durability. SSVs are independent of structure in quartzites and the results lying below 5% are suitable for ballasts (AREMA, 2009).

***Los Angeles abrasion value***

The LAA test determines the hardness property of aggregates. It measures the abrasion resistance of aggregates (ASTM C535, 2016). Los Angeles abrasion value (LAAV) of quartzite ranges from 12.07% (as in F7) to 31.34% (as in F2) (Table 8). The variation of LAAV seems to be independent of shape indices and physical properties such as dry density of ballasts (Fig. 9). All the quartzite particles tested are of angular to subangular shape because all the samples are crushed aggregate. Therefore, angular shape does not indicate much bearing on LAAV. However, with increased roundness of fresh ballasts, the degree of Los Angeles abrasion tends to decrease (Okonta, 2015). It is as opposed to results of Guo et al. (2018).

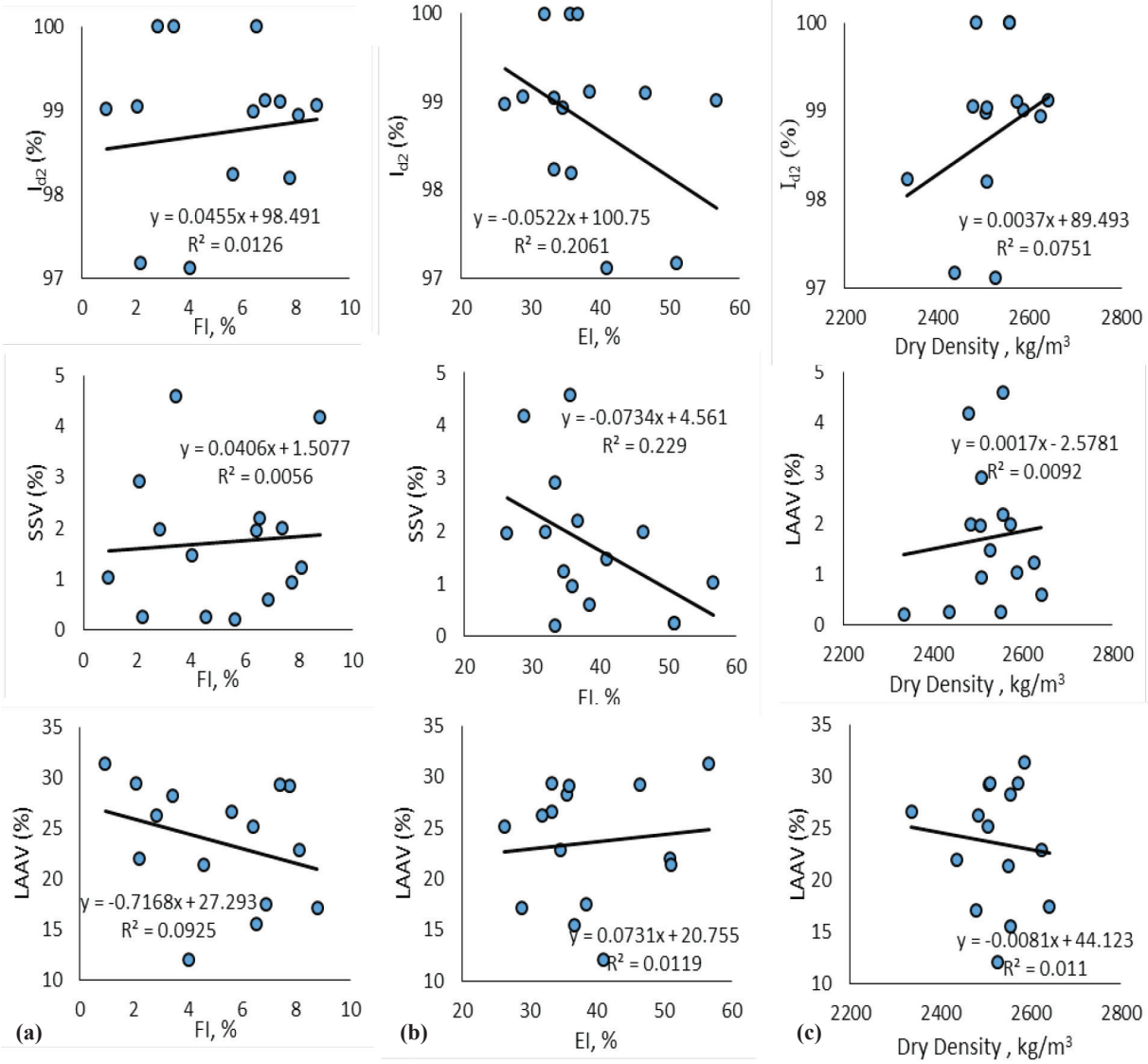


**Fig. 9: Relationships of durability with shape indices and dry density of quartzite. (a) Flakiness index (FI) index versus durability parameters, (b) elongation index (EI) versus durability parameters, (c) dry density versus durability parameters.**

They found flaky and elongated particles to be worn out more readily loosing volume of particles under abrasion test. Present study shows that the quartzite is less flat and slightly appreciably elongated. Even under such condition, there is weak influence of EI and FI on durability against abrasion presumably due to good interlocking of grains in quartzite. Sekine et al. (2005) also indicate that relationships between shape and strength diminish as the stiffness of ballasts increases.

LAAV of quartzite has also very weak correlation with AIV, ACV and PLSI (Fig. 10). However found good negative correlation between LAAV and PLSI for carbonate rocks. Therefore, the relationships perhaps rely on rock types.

Out of fifteen samples only F2 has exceeded LAAV of 30% and seven samples have LAAV lying below 25% of which four samples have <20%. The majority of the samples fall into the acceptable limit of <35% suggested by AREMA (2009).

***Comparison among quartzites of previous and present studies***

Except for the similarity of the rock type of the Fagfog Quartzite studied previously and at present, other quartzites of the previous studies are different from the Fagfog Quartzite. Quartzite studied by Bista and Tamrakar (2015) and Tumbapo (2016) are comparable in terms of age and types (Table 9). Density of the Fagfog Quartzite studied at present comes to vary within a comparable range compared to the earlier studies (Abdullah and Singh, 2010; Gupta and Singh, 2012; Paudel and Tamrakar, 2013; Bista and Tamrakar, 2015; Tumbapo, 2016; Singh et al., 2017). Specific gravity and water absorption are also quite comparable with the results of the previous studies (Abdullah and Singh, 2010; Paudel and Tamrakar, 2013; Adom-Asamoah, 2014; Woode et al., 2015; Bista and Tamrakar, 2015; Tumbapo, 2016) of similar and different quartzites (Table 9). The bulk density of the Fagfog quartzite is lower compared to that of quartzites determined by Shareef (2015).

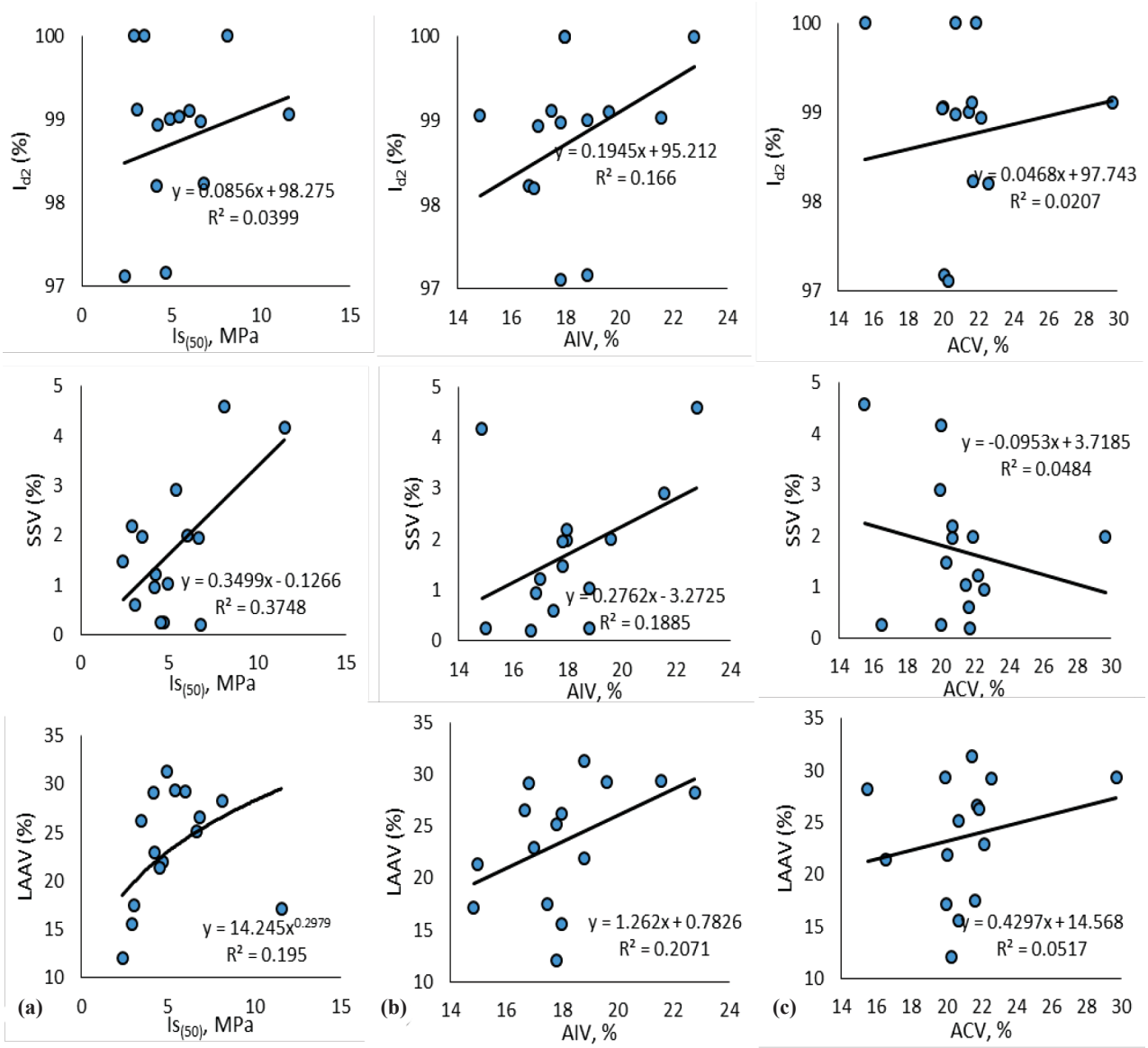


**Fig. 10: Relationships between durability and strength parameters. (a) Point-load strength index versus durability parameters, (b) AIV versus durability parameters, (c) ACV versus durability parameters.**

**Table 7: Result of magnesium sulphate soundness test of ballasts from the Fagfog Quartzite.**

| Sample No. | Initial wt. (kg) | 1st cycle wt. after immersion in $MgSO_4$ and drying in oven (kg) | 2nd cycle wt. after immersion in $MgSO_4$ and drying in oven (kg) | 3rd cycle wt. after immersion in $MgSO_4$ and drying in oven (kg) | 4th cycle wt. after immersion in $MgSO_4$ and drying in oven (kg) | 5th cycle wt. after immersion in $MgSO_4$ and drying in oven (kg) | Wt. after washing with $BaCl_2$ solution (kg) | SSV% |
|---|---|---|---|---|---|---|---|---|
| F1 | 2.000 | 2.010 | 2.015 | 2.025 | 2.025 | 2.020 | 1.996 | 0.20 |
| F2 | 2.035 | 2.050 | 2.050 | 2.050 | 2.050 | 2.050 | 2.014 | 1.03 |
| F3 | 2.005 | 2.015 | 2.020 | 2.020 | 2.020 | 2.020 | 2.000 | 0.25 |
| F4 | 2.015 | 2.020 | 2.020 | 2.015 | 2.015 | 2.015 | 2.003 | 0.60 |
| F5 | 2.070 | 2.075 | 2.085 | 2.085 | 2.075 | 2.055 | 1.975 | 4.59 |
| F6 | 2.005 | 2.015 | 2.025 | 2.030 | 2.030 | 2.025 | 2.000 | 0.25 |
| F7 | 2.035 | 2.045 | 2.045 | 2.035 | 2.035 | 2.030 | 2.005 | 1.47 |
| F8 | 2.110 | 2.120 | 2.130 | 2.130 | 2.130 | 2.125 | 2.090 | 0.95 |
| F9 | 2.010 | 2.035 | 2.045 | 2.050 | 2.045 | 2.015 | 1.970 | 1.99 |
| F10 | 2.020 | 2.060 | 2.050 | 2.040 | 2.040 | 2.040 | 1.980 | 1.98 |
| F11 | 2.050 | 2.085 | 2.075 | 2.070 | 2.070 | 2.060 | 2.010 | 1.95 |
| F12 | 2.040 | 2.080 | 2.070 | 2.070 | 2.065 | 2.070 | 2.015 | 1.23 |
| F13 | 2.035 | 2.050 | 2.055 | 2.050 | 2.055 | 2.055 | 1.950 | 4.18 |
| F14 | 2.055 | 2.060 | 2.065 | 2.065 | 2.060 | 2.035 | 2.010 | 2.19 |
| F15 | 2.060 | 2.065 | 2.070 | 2.070 | 2.050 | 2.040 | 2.000 | 2.91 |

**Table 8: Los Angeles Abrasion Value (LAAV) of the Fagfog Quartzite.**

| Sample No. | Initial mass passing 50 mm and retained on 37.5 sieves (kg) | Initial mass of sample passing 37.5 mm and retained on 25 mm sieves (kg) | Total mass of test sample (kg) | Wt. retained on 1.7 mm sieve after 1000 revolution (kg) | Loss in wt. (kg) | LAAV (%) |
|---|---|---|---|---|---|---|
| F1 | 5.045 | 5.005 | 10.050 | 7.380 | 2.670 | 26.57 |
| F2 | 5.02 | 5.03 | 10.050 | 6.335 | 3.150 | 31.34 |
| F3 | 5.075 | 5.045 | 10.120 | 7.900 | 2.220 | 21.94 |
| F4 | 5.065 | 5.04 | 10.105 | 8.340 | 1.765 | 17.47 |
| F5 | 5.035 | 5.04 | 10.075 | 7.230 | 2.845 | 28.24 |
| F6 | 5.19 | 5.075 | 10.265 | 8.070 | 2.195 | 21.38 |
| F7 | 5.13 | 5.185 | 10.315 | 9.070 | 1.245 | 12.07 |
| F8 | 5.05 | 5.03 | 10.080 | 7.140 | 2.940 | 29.17 |
| F9 | 5.035 | 5.05 | 10.085 | 7.130 | 2.955 | 29.30 |
| F10 | 5.195 | 5.06 | 10.255 | 7.565 | 2.690 | 26.23 |
| F11 | 5.09 | 5.155 | 10.245 | 7.665 | 2.580 | 25.18 |
| F12 | 5.02 | 5.5 | 10.520 | 8.112 | 2.408 | 22.89 |
| F13 | 5.06 | 5.015 | 10.075 | 8.350 | 1.725 | 17.12 |
| F14 | 5.18 | 5.095 | 10.275 | 8.680 | 1.595 | 15.52 |
| F15 | 5.165 | 5.045 | 10.210 | 7.210 | 3.000 | 29.38 |

**Table 9: Physical, mechanical and durability properties of some quartzites compared with the present study**

| | | Abdullah and Singh (2010) | Gupta and Sharma (2012) | Paudel and Tamrakar (2013) | Adom-Asamoah et al. (2014) | Woode et al. (2015) | | Shareef (2015) | Bista and Tamrakar (2015) | Tumbapo (2016) | Singh et al. (2017) | Present study |
|---|---|---|---|---|---|---|---|---|---|---|---|---|
| | Rocktype | Metaquarzite | Pandukeshwar Quartzite; Tapovan Quartzite; Berinag Quarrzite | Chisapani Quarzite Pandrang Quarzite | Metaquarzite | Schistose Quartzite | Massive Metaquartzite | Quartzite | Fagfog Quartzite; Purbensi Quartzite; Dunga Quartzite; Chisapani Quartzite | Dunga Quartzite; Pandrang Quartzite; Chisapani Quartzite | Phyllitic Quartzite | Fagfog Quartzite |
| | Colour | Grey purple colour | | white, yellowish white | dark purple reddish brown | Brn., D brn., Cream | Brn., D brn., Cream | | Pink, yellow-grey; grey-yell grey; grey; light grey | White; greyish white; white | Dark grey | White, yellowish white, brownish white |
| | Geological Age | Pre cambrian | Proterozoic; Paleoproterozoic; Neoproterozoic | Pre cambrian | Precambrian | Neoproterozoic; Togo Formation | | Quaternary Fluvial Deposit | Precambrian; Precambrian; Early Paleozoic; Precambrian | Early Paleozoic; Precambriran; Precambrian | Neoproterozoic | Precambrian |
| Physical Properties | EI, % | | | | | | | | | | | 0.92-8.80 |
| | FI, % | | | | 14-19 | | | | | | | 28.85-56.68 |
| | Density, Kg/m$^3$ | 2677 | 2710; 2660; 2690 | 2560; 2590 | | | | | 2640-2730; 2730-2850; 2670; 2660 | 2520-2670;2520-2640; 2570-2690 | 2690 | 2336-2641 |
| | Sp gr | | | | | | | | 2.57-2.70; 2.68-2.81; 2.66; 2.65 | | 2.77 | 2.34-2.65 |
| | WA, % | 0.2 | | 0.40; 0.35 | 1.0-2.0 | 0.39 | 0.31 | 0.55 | 0.32-0.90; 0.56-0.64; 0.15; 0.22 | 0.22-0.38; 0.29-0.46; 0.21-0.46 | | 0-2.50 |
| | Bulk Density, kg/m$^3$ | | | | | | | 1519 | | | | 1204-1387 |
| Strength Measures | PLS, MPa | | | | | | | | 5.50-6.47; 2.18-2.97; 1.25; 6.49 | 3.52-6.45; 2.93-3.78; 1.63-7.13 | | 2.40-11.55; |
| | UCS, MPa | 75 | 99; 79; 90 | 189;140 | 116-311 | | | | 126-149; 50-68; 29; 149 | 61-110; 32-118; 41-122 | 106 | 39-302 |
| | AIV, % | | | 22.64;22.64 | 8.0-19 | 19.49 | 15.3 | | 10.94-20.12; 10.60-11.66; 16.70-23.26; 10.48 | | | 14.85-22.77 |
| | ACV, % | | | 24.66;25.66 | 16-19 | 31.4 | 17.75 | | | | | 15.51-29.70 |
| Durability | SDI (Id2), % | | | | | | | | | | 99.35 | 96.94-100 |
| | Magnesium SSV, % | | | 12.08;12.55 | | | | | Sodium SSV: 4.91-7.51; 4.64; 5.50-10.71; 5.78 | | | 0.20-4.59 |
| | LAAV, % | | | | 29-46 | 38.75 | 27.45 | | 47.5 (Fagfog Quartzite); 21.18 (Nourpur Formation) | 23-53; 24-35; 38-40 | | 12.07-31.34 |

Point-load strength index of the Fagfog Quartzite varies within a wider range compared to the results of the earlier studies (Bista and Tamrakar, 2015; Tumbapo, 2016). UCS of the current study is wider in range compared to the range obtained by Bista and Tamrakar (2015). Majority of quartzites gave less than 150 MPa except of higher values around 300 Mpa (Adom-Asamoah et al., 2014; present study, Table 9). This variation occurred could be due to consideration of greater number of samples at present study, variation of locality of sampling and types of samples conpared to Paudel and Tamrakhar (2013), and Bista and Tamrakar (2015). It does not differ with AIV of other quartzites (Woode et al., 2015), but Adom-Asamoah et al. (2014) obtained as low as 8%. ACV of the current study (Table 9) is similar to that of quartzites studied by Woode et al. (2015), Paudel and Tamrakar (2013) and Adom-Asamoah et al. (2014).

Slake durability index of quartzites vary within narrow range (Singh et al., 2017; Table 9), and generally quartzites have high values of SDI. Sodium SSV of the Fagfog Quartzite (Bista and Tamrakar, 2015) is slightly higher than the magnesium SSV of the Fagfog Quartzite (Table 9).

LAAV of the Fagfog Quartzite varies between 12.07 and 31.34% which is quite lesser than the result obtained by Bista and Tamrakar (2015) for the Fagfog Quartzite, and by Adom-Asamoah et al. (2014), Woode et al. (2015) and Tumbapo (2016) for other quartzites.

## CONCLUSIONS

All the quartzite samples belong to the lithostratigraphic unit: Fagfog Quarzite from the Lower Nawakot Group of Precambrian age. Quartzites are medium-grained massive to laminated, with dominantly of well interlocked quartz grains. The rock fabric indicate recrystallization microstructure of low to intermediate temperature where biotite appears.

The ballast particles are all crushed quartzite which have low flakiness index but with slightly large elongation index. Specific gravity and apparent dry density of the ballast samples vary between 2.38 and 2.70, and between 2433.95 kg/m$^3$ and 2809.86 kg/m$^3$, respectively. Bulk density of the samples varies from 1203.62 kg/m$^3$ to 1386.88 kg/m$^3$. Therefore, the ballast are normal weight aggregates. PLSI of quartzite varies from 2.40 to 11.4 MPa. The quartzites are moderately strong to extremely strong. with AIV below 22% and ACV 30% below.

The quartzite samples have yielded high to very high slake durability indices indicating that they are durable against slaking. There was no significant change in slake durability index from the second to the fifth cycles, because reduction of 1 to 2 percent occurred. Regarding deterioration, half of samples deteriorated with type I and the remaining half with type II. About one third of samples have shown deterioration of type II after the fifth cycle. After the fifth cycle no sample showed deterioration of type III.

The magnesium SSV and LAAV obtained for quartzites represent that the quartzite samples are suitable for railway track ballast suggested by AREMA (2009). The AIV and ACV show strong and satisfactory to resistance to impact and crushing loads for ballast aggregate.

The correlations between shape and density with durability, and durability and strength parameters are found to be weak to very weak.

The results of physical properties, and strength and durability parameters obtained for the Fagfog Quartzites are comparable with range of results obtained for different quartzites in earlier studies. Some variation of the values are probably owing to the change in locality of sampling, rock state of weathering, and some inherent variation among quartzites.

## ACKNOWLEDGEMENTS

Authors are thankful to Central Department of Geology, Tribhuvan University, Institute of Engineering (IoE), and Department of Mines and Geology (DMG) for providing laboratory facilities. D. Shrestha, J. B. Gurung, and S. Ranabhat are thanked for their assistance in fieldwork and S. Pradhananga and S. Maharjan are thanked for their assistance in laboratory testing.

## REFERENCES

Abdullah, H. and Singh, S., 2010, Laboratory Evaluation of Five Quartzites. Indian Geotechnical Conference, IGS Mumbai Chapter and IIT Bombay, pp. 263–266.

Adom-Asamoah, M., Tuffour, Y. A., Afrifa, A. O., and Kankam, C. K., 2014, Strength Characteristics of Hand-Quarried Partially-Weathered Quartzite Aggregates in Concrete. American Journal of Civil Engineering, v. 2(5), pp. 134–142.

Ahmada, M., Ansaria, M. K., Sharma, L. K., Singh, R., and Sinha, T. N., 2017, Correlation between strength and durability indices of rocks-soft computing approach, v. 191, pp. 458–466.

AREMA: Manual for Railway Engineering, 2010, Vol. 1: Track, Ch. 1: Roadway and Ballast, American Railway Engineering and Maintenance of Way Association (AREMA).

ASTM C 127, 2011, Standard Test Method for Density, Relative Density (Specific Gravity), and Absorption of Coarse Aggregate. ASTM International, West Conshohocken, PA, 2011, DOI: 10.1520/C0127-11, www.astm.org.

ASTM C535, 2016, Standard test method for resistance to degradation of large-size coarse aggregate by abrasion and impact in the Los Angeles machine. ASTM Standards ASTM International, West Conshohocken, PA, https://www.astm.org/Standards/C535.htm

ASTM D4644-87, 1992, Standard Test Method for Slake Durability of Shales and Similar Weak Rocks. ASTM International, West Conshohocken, PA, 2011, DOI: 10.1520/D04644-92.

ASTM D5731–02, 2003, Standard Test Method for Determination of the Point Load Strength Index of Rock. ASTM International, West Conshohocken, PA.

ASTM C88-05, 2005, Standard test method for Soundness of Aggregates by use of sodium sulphate or magnesium sulphate. ASTM International, Standard test method for Soundness of Aggregates by use of sodium sulphate or magnesium sulphate. C88-05, pp. 1–5.

ASTM C 29/C 29M – 07, 2007, Standard Test Method for Bulk Density (Unit Weight) and Voids in Aggregate. ASTM International. 5 p.

Bista, K. and Tamrakar, N. K., 2015, Evaluation of strength and durabililty of rocks from Malekhu-Thopal Khola area, central Nepal Lesser Himalaya for construction aggregates. Bull. Dept. Geol., Tribhuvan University, Kathmandu, Nepal, v. 18, pp. 15–34.

Broch, E. and Franklin, J. A., 1972, The point-load strength test. International journal of rock mechanics and mining sciences, v. 9, pp. 669–697.

BS 812-105.1, 1989, Methods for determination of particle shape-Section 105.2 Flakiness index. British Standard Institution. 8 p.

BS 812-105.2, 1989, Methods for determination of particle shape-Section 105.1 Elongation index. British Standard Institution. 12 p.

BS 812-110, 1990, Testing aggregates Methods for determination of aggregate crushing value (ACV). British Standard Institution.

BS 812-112, 1990, Testing aggregates Method for determination of aggregate impact value (AIV). British Standard Institution.

BS EN13450, 2013, Aggregates for Railway Ballasts. British Standard Institution Standards Limited. 38 p.

Erguler, Z. A. and Ulusay, R., 2009, Assessment of physical disintegration characteristics of clay-bearing rocks: Disintegration index test and a new durability classification chart. Engineering Geology, v. 105, pp. 11–19.

Fereidooni, D. and Khajevand, R., 2017, Correlations between slake durability index and engineering properties of some travertine samples under wetting-drying cycles. Geotechnical and Geological Engineering. v. 36(6), pp. 1071–1089.

Gautam, T. P. and Shakoor, A., 2013, Slaking behavior of clay-bearing rocks during a one-year exposure to natural climatic conditions. Engineering Geology, v. 166, pp. 17–25.

Gökçeoğlu, C., Ulusay, R., and Sönmez, H., 2000, Factors affecting the durability of selected weak and clay bearing rocks from Turkey, with particular emphasis on the influence of the number of drying and wetting cycles. Engineering Geology, v. 57, pp. 215–237.

Guo, Y., Markine, V., Song, J., and Jing G., 2018, Ballast degradation: Effect of particle size and shape using Los Angeles Abrasion test and image analysis. Construction and Building Material, v. 169, pp. 414–424.

Gupta, V. and Sharma, R., 2012, Relationship between textural, petrophysical and mechanical properties of quartzites: A case study from northwestern Himalaya. Engineering Geology, v. 125-136, pp. 1–9.

IRS-GE-1, 2004, Specifications for track ballast (ISSUE-1), https://ecr.indianrailways.gov.in/uploads/files/1366518435624-GE-IRS-1.pdf

IRS-GE-1, 2016, Specifications for track ballast, Research Designs and Standards Organization (RDSO). Ministry of Railways.

ISRM, 1979, Suggested methods for determining the uniaxial compressive strength and deformability of rock materials, Int. Jour. Rock Mech. Min. Sci., 16(2), 135–140.

ISRM, 1981, Suggested methods for the rockcharacterization, testing and monitoring, ISRMCommission on Testing Methods. Brown, E.T. (Ed.) Opergaom Press.

Khanal, S. and Tamrakar, N., 2009, Evaluation and quality of crushed-limestone and siltstone for road aggregates. Bull. Dept. Geol., v. 12, pp. 29–42.

Maharjan, D. K. and Tamrakar, N. K., 2003, Quality of siltstone for concrete aggregates from Nallu Khola area Kathmandu, Nepal. Jour. Geol. Soc., v. 30, pp. 167–176.

Maharjan, S. and Tamrakar, N. K., 2007, Evaluation of gravel for concrete and road aggregates, Rapti River, central Nepal SubHimalaya. Bull. Dept. Geol., Tribhuvan University, Kathmandu, Nepal, v. 10, pp. 99–106.

Okonta, F. F., 2015, Effect of grading category on the roundness of degraded and abraded railway quartzites. Engineering Geology, 193(1), pp. 231–242.

Paudel, P. N. and Tamrakar, N.K., 2013, Physical, mechanical and petrographic properties of Lesser Himalayan rocks from Kavre area: An assessment of quality for concrete aggregate. Jour. Nepal Geol. Soc., v. 46, pp. 199–210.

Sekine, E., Kono, A., and Kito, A., 2005, Strength and deformation characteristics of reailroad ballasts in ballast particle abrasion process. Quarterly Report of RTRI, v. 46(4), pp. 256–261.

Shareef, U., 2015, Study on Physical and Mechanical Properties of Quartzite and Silico-Manganese Slag As Alternative Material for Coarse Aggregate. International Journal for Scientific Research and Development, v. 3(9), pp. 72–74.

Singh, T., Jain, A., and Rao, K. S., 2017, Physico-mechanical Behaviour of Metamorphic Rocks in Rohtang Tunnel, Himachal Pradesh, India. Procedia Engineering, v. 191, pp. 419–425.

Stipp, M., Stinitz, H., Heilbronner, R., and Schmid, S.M., 2002, The eastrn Tonale fault zone: a 'natura laboratory' for crystal plastic deformation of quartz over a temperature range from 250 to 700oC. Journal of Structural Geology, v. 24, pp. 1861–1884.

Stöcklin, J., 1980, Geology of Nepal and its regional frame. Jour. Geol. Soc., London, v. 137, pp. 1–34.

Stöcklin, J. and Bhattarai, K. D., 1977, Geology of the Kathmandu area and central Mahabharat range, Nepal Himalaya. Report of Department of Mines and Geology/ United Nation Development Program (unpublished), 86 p.

Tamrakar, N. K., Yokota, S., and Shrestha, S. D., 2002, Physical and geomechanical properties of the Siwalik sandstones, Amlekhganj-Suparitar area, central Nepal Himalaya. Journal. Nepal Geological. Society, v. 26, pp. 59–71.

Tumbapo, P., 2016, Rock mass characteristics and engineering properties of quartzites of the Lesser Himalaya, Suparitar-Dhorsing area, Makawanpur District, central Nepal. Unpublished M. Sc. Thesis submitted to Central Department of Geology, Tribhuvan University, Kirtipur, Kathmandu, Nepal, 86 p.

Woode, A. Amoah, D. K., Aforia, B., Avor, F., and Kissi, F. K., 2015, Engineering Geological Characteristics of Quartzite Types for Concrete Production in Ghana. Civil and Environmental Research. Civil and Environmental Research, v. 7(10), pp. 6–11.